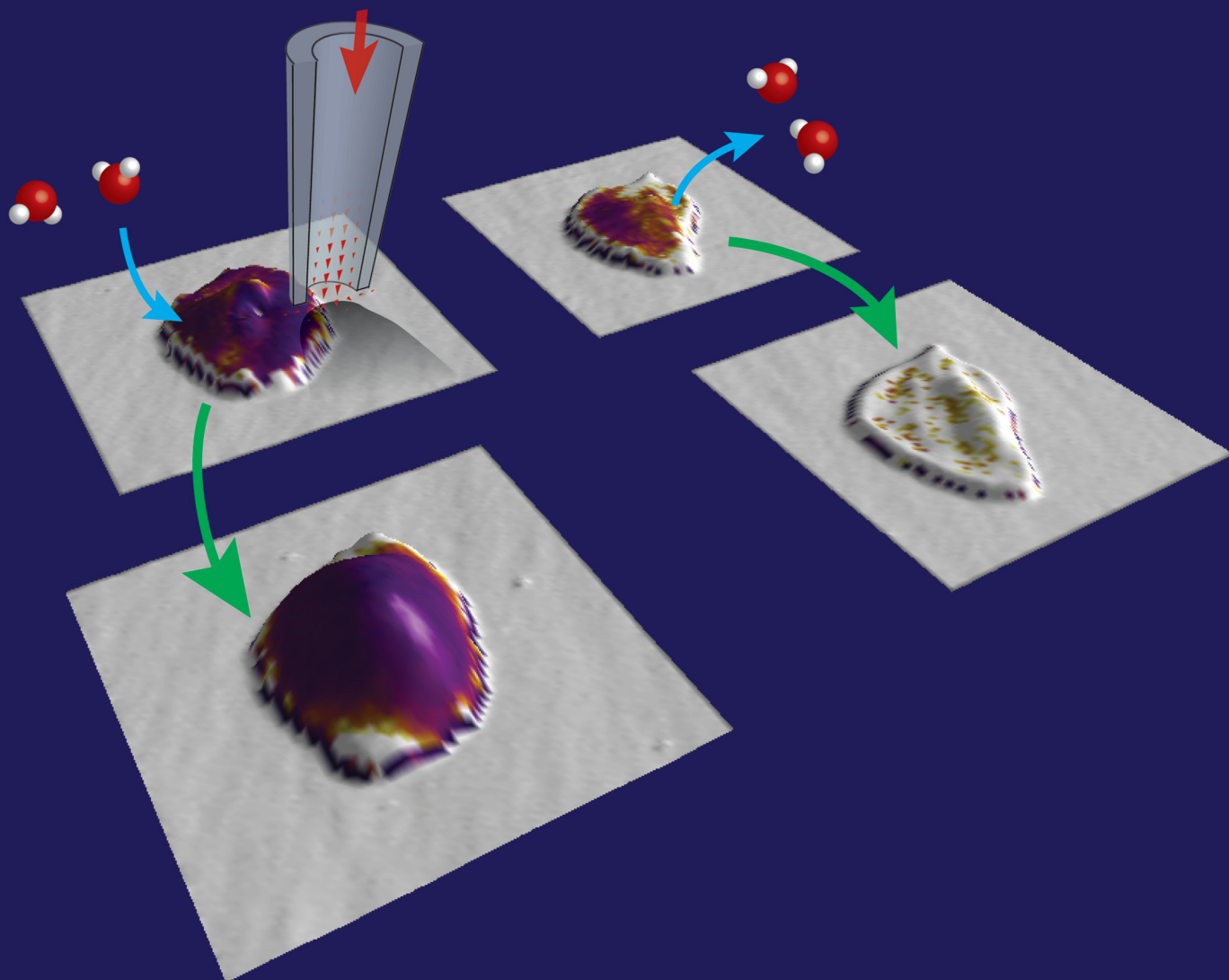


# Soft Matter

rsc.li/soft-matter-journal



ISSN 1744-6848

**PAPER**

Johannes Rheinlaender *et al.*  
Platelet stiffness correlates inversely with platelet volume  
during expansion and compression



Cite this: *Soft Matter*, 2026, **22**, 578

## Platelet stiffness correlates inversely with platelet volume during expansion and compression

Konstantin Krutzke, <sup>a</sup> Jan Seifert, <sup>a</sup> Meinrad Gawaz, <sup>b</sup> Tilman E. Schäffer <sup>\*a</sup> and Johannes Rheinlaender <sup>\*a</sup>

The stiffness and the volume of human platelets change under various conditions, affecting their function and viability. Although the influence of platelet volume on platelet function in health and disease has been extensively studied, the relationship between volume and stiffness – in contrast to many other cell types – remains unexplored for platelets, probably due to the difficulty in measuring platelet mechanics as platelets tend to activate under stress. Here, we investigate the relationship between platelet volume and stiffness using scanning ion conductance microscopy (SICM). SICM can image the topography and therefore quantify the volume as well as measure the mechanical properties of living cells under physiological conditions with submicrometer resolution. We found a link between platelet stiffness and volume changes caused by water efflux/influx due to osmotic compression/expansion at the single cell level. With increasing platelet volume, the stiffness decreased and *vice versa*. We then confirmed this inverse relationship by measurements of platelets during two additional, physiologically highly relevant situations: The dynamic spreading of platelets on a surface and platelets subjected to a spatial confinement, where a decrease in volume was also accompanied by an increase in stiffness and platelets subjected to spatial confinement showed a significantly larger volume compared to unconfined platelets, with a correspondingly lower stiffness, respectively. In conclusion, our SICM analysis revealed a universal, inverse correlation between platelet stiffness and volume change, opening up new perspectives in platelet research.

Received 17th August 2025,  
Accepted 12th November 2025

DOI: 10.1039/d5sm00839e

[rsc.li/soft-matter-journal](http://rsc.li/soft-matter-journal)

### Introduction

Platelets are one of the three types of mammalian blood cells and are involved in hemostasis and thrombosis.<sup>1–4</sup> Upon vessel injury, platelets get activated and adhere to the extracellular matrix, such as collagen or fibrinogen.<sup>5,6</sup> This induces a signaling cascade that releases biochemical compounds to bind more platelets to the site of the injury.<sup>7–9</sup> A key aspect of this process is platelet stiffness, which is determined by their cytoskeleton<sup>10–12</sup> and is essential for their function and viability.<sup>6,13</sup>

For many eukaryotic cells it has been reported that stiffness is directly related to volume. This relationship remains consistent regardless of different mechanical state, biochemical treatment, or cellular confinement.<sup>14,15</sup> Understanding changes in cell volume and the resulting alterations in cell stiffness are essential in biomedical research, as these parameters reflect

fundamental aspects of cellular physiology and biomechanics, influencing cellular functions such as division, intracellular transport,<sup>16</sup> differentiation,<sup>17</sup> signaling,<sup>18</sup> and response to environmental stimuli.<sup>15,19,20</sup> Moreover, cell volume and stiffness play critical roles in pathophysiological conditions, offering insights into disease mechanisms and potential therapeutic targets.<sup>21–23</sup> In the context of platelets, exploring their volume and stiffness provides valuable insights into their unique physiology. For example, platelets undergo dynamic changes in shape and volume during activation, which are essential for their hemostatic function.<sup>24,25</sup> The mechanical adaptation of platelets plays an important role during adhesion, activation, aggregation, and migration.<sup>26–28</sup> Studying this adaptation behavior may therefore reveal new aspects of platelet functionality and contribute to understanding disorders related to thrombosis.<sup>3,29</sup> However, so far, no relationship between stiffness and volume has been reported for platelets.

In this study, we use scanning ion conductance microscopy<sup>30,31</sup> (SICM) to measure platelet volume<sup>32</sup> as well as platelet stiffness without any physical contact of the probe with the sample.<sup>26,27</sup> SICM has been increasingly applied in the investigation of various aspects of platelet biology, including their adhesion,<sup>33</sup> morphology,<sup>32</sup> mechanical properties,<sup>26</sup> migration

<sup>a</sup> Institute of Applied Physics, University of Tübingen, Auf der Morgenstelle 10, 72076, Tübingen, Germany. E-mail: [tilman.schaeffer@uni-tuebingen.de](mailto:tilman.schaeffer@uni-tuebingen.de), [johannes.rheinlaender@uni-tuebingen.de](mailto:johannes.rheinlaender@uni-tuebingen.de); Fax: +49 7071 295093; Tel: +49 7071 2976030

<sup>b</sup> Department of Internal Medicine III, Cardiology and Angiology, University of Tübingen, Germany



behavior,<sup>27</sup> roles in thrombosis,<sup>34</sup> and volume dynamics,<sup>35</sup> providing new insights into platelet function and pathology, especially single-platelet biomechanics<sup>36</sup> and the platelet cytoskeleton.<sup>12</sup> Using time-resolved SICM imaging, we show that platelets soften upon osmotic swelling and stiffen upon osmotic shrinkage, following a general inverse correlation between relative volume and stiffness observed previously for many other cell types.<sup>14,15,37</sup> We then investigated two further physiologically relevant situations, platelets dynamically spreading on a surface and platelets subjected to spatial confinement. In both situations, the same inverse correlation was observed. Thus, we demonstrate that this inverse correlation between volume and stiffness appears to be a fundamental property of living platelets.

## Methods

### Human platelet isolation and preparation

Platelets were isolated as described previously.<sup>38</sup> Briefly, venous blood was drawn from healthy volunteers with informed consent. All procedures were performed in compliance with relevant laws, followed institutional guidelines, were approved by the institutional ethics committee (273/2018BO2), and are consistent with the Declaration of Helsinki. To prevent coagulation, acid citrate dextrose (in a 1:4 ratio) was filled into monovettes (04.1926.001, Sarstedt, Nümbrecht, Germany) before blood was drawn. First the monovettes were centrifuged at  $200 \times g$  for 20 min and platelet-rich plasma (PRP) was collected. The PRP was transferred to Tyrode-HEPES buffer (in a 1:3 ratio) (136.89 mM NaCl, 2.81 mM KCl, 11.9 mM NaHCO<sub>3</sub>, 1.05 mM MgCl<sub>2</sub>, 0.42 mM NaH<sub>2</sub>PO<sub>4</sub>, 5.56 mM D-glucose, 1 g L<sup>-1</sup> BSA, 4 mM HEPES) pH 6.5. After another centrifugation at  $880 \times g$  for 10 min, platelets were then carefully resuspended in 1 mL of isotonic Tyrode-HEPES buffer (isotonic osmolarity: 295 mOsmol L<sup>-1</sup>) pH 7.4.

The topography as well as the stiffness of isolated platelets were measured with SICM (see below). For that, unless otherwise noted, platelets (100  $\mu$ L of suspension) were added to a cell culture dish (627160, Greiner Bio-One GmbH, Kremsmünster, Austria) for 10 s followed by three washing steps using isotonic Tyrode-HEPES buffer, pH 7.4, to remove all non-adhered platelets. The remaining adhered platelets were allowed to spread for 10 min. Then, the SICM measurements were carried out. To investigate the possible influence of surface coating or platelet spreading area, platelets were also prepared on fibrinogen-coated (fibrinogen from human plasma, F1056, Sigma Aldrich, Missouri, USA, 20  $\mu$ g mL<sup>-1</sup> in H<sub>2</sub>O, 15 min at 37 °C) or non-coated cell culture dishes (627161, Greiner Bio-One).

To investigate spreading platelets, 10  $\mu$ L of platelet suspension was diluted in isotonic Tyrode-HEPES buffer with 0.1 U mL<sup>-1</sup> thrombin (T6884-250UN, Sigma Aldrich), then adding the thrombin-treated platelets to a cell culture dish (627160, Greiner Bio-One), which was then mounted into the SICM setup. Subsequently, spreading platelets were optically selected

by phase contrast microscopy and then imaged with SICM for at least 20 min.

To measure spatially confined platelets, platelets were activated with 0.1 U mL<sup>-1</sup> thrombin for 30 s and then added to the microcontact-printed cell culture dishes (see below) for an additional 10 min incubation at 37 °C. The cell culture dish was then washed three times with fresh isotonic Tyrode-HEPES buffer and platelets could spread for another 15 min at 37 °C. The following SICM measurements were achieved by mounting the cell culture dishes into the SICM setup and fibrinogen lines were identified using the TRITC HC filter set (F36-503, AHF Analysentechnik AG, Tübingen, Germany).

To investigate the influence of the actin cytoskeleton, adherend platelets were treated with cytochalasin D (cytoD) during SICM imaging. For that, cytoD (Cay11330-5, Cayman Chemical Company, Michigan, USA, solved at 10 mM in DMSO) was added at a final concentration of 10  $\mu$ M to the Tyrode-HEPES buffer 10 min before ( $t = -10$  min) the induction of a hypotonic/hypertonic shock (at  $t = 0$  min, 412 or 177 mOsmol L<sup>-1</sup>).

### Cell culture

The preparation of MEF cells for SICM measurements was carried out as follows. The existing medium in the cell culture flask was completely removed, and the entire flask was washed three times with phosphate-buffered saline (PBS, D8537, Sigma Aldrich) at 37 °C. Then, trypsin/EDTA (T3924, Sigma Aldrich) was added to the cell culture flask and placed in the incubator at 37 °C for *ca.* 2 min. After gently tapping the flask bottom, all adherent cells were detached. Subsequently, Dulbecco's modified Eagle's medium (DMEM, D5030, Sigma Aldrich), supplemented with 10% (v/v) fetal calf serum, 1% (v/v) penicillin-streptomycin, and 1% (v/v) L-glutamine (200 mM), was added to the cell culture flask, the entire contents were transferred to a centrifuge tube, and centrifuged at *ca.* 270 g for 5 min. The remaining medium was removed and discarded, and the pellet was resuspended in medium. The cell suspension was diluted 1:10 and added to a cell culture flask (627160, Greiner Bio-One) with medium and placed in the incubator at 37 °C for at least 12 hours before using the cells for SICM measurement. To prepare cells for measurement, they were first washed three times with PBS (37 °C), followed by the addition of CO<sub>2</sub>-independent medium (Leibovitz L15 Medium, 21083027, Thermo Fisher Scientific Inc., Massachusetts, USA) to the cell culture dish, and then placed in the SICM setup.

### Scanning ion conductance microscopy (SICM)

To investigate platelet volume and stiffness, self-built SICM setups were used.<sup>26,35</sup> Electrolyte-filled nanopipettes with inner opening radii of typically 80–100 nm for platelets (validated by scanning electron microscopy, Fig. 1A, inset) and typically 200 nm for MEF cells were manufactured from glass capillaries (1B100F-4, World Precision Instruments Inc., Sarasota, FL, USA) using a CO<sub>2</sub>-laser based pipette puller (P2000, Sutter Instruments, California, USA). A voltage of 250 mV was applied between two electrodes, one inside the pipette and one outside the pipette in the electrolyte-filled cell culture dish, to induce a



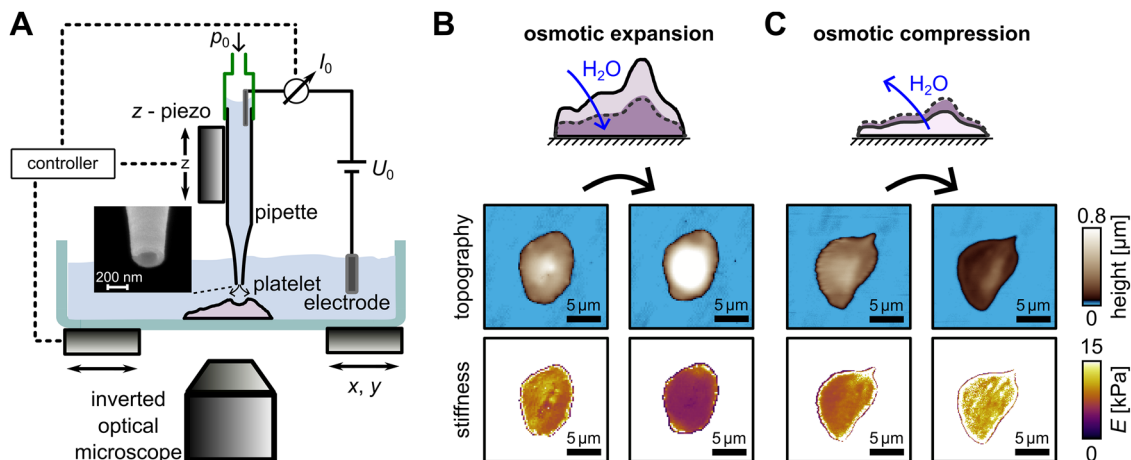


**Fig. 1** Measuring platelet topography and stiffness with SICM. (A) Schematic of a SICM setup. A bias voltage  $U_0$  is applied between two electrodes, which induces an ion current  $I_0$  through an electrolyte-filled nanopipette. A pressure  $p_0$  is applied to the nanopipette to measure the mechanical stiffness of the sample. (B) and (C) Topography and stiffness images of platelets before (left) and after (right) osmotic expansion ((B),  $t = 1$  min after hypotonic shock, osmolarity:  $147 \text{ mOsmol L}^{-1}$ ) or compression ((C),  $t = 1$  min after hypertonic shock, osmolarity:  $495 \text{ mOsmol L}^{-1}$ ).

distance-sensitive ion current through the tip of the pipette, which typically results in an ion current in the range of 6–8 nA. To measure stiffness, a constant pressure  $p_0$  of 10 kPa for platelets or 5 kPa for MEF cells was applied to the upper end of the nanopipette and the ion current as a function of the vertical position ( $Iz$ -curves) with a trigger setpoint of 98% of the saturation current  $I_0$  were recorded on a raster-pattern with typically  $40 \times 40$  pixels. The pixel resolution was chosen to roughly match the physical resolution of the topography imaging<sup>39</sup> and stiffness mapping<sup>40</sup> and gives a precision of the platelet volume measurement of typically 1%.<sup>35</sup> An approach speed of  $80 \mu\text{m s}^{-1}$ , a retract speed of  $400 \mu\text{m s}^{-1}$ , and reduced pixel number on the substrate were used, which resulted in typically 30 s per frame. The stiffness was then calculated from the slope of the  $Iz$  curves between 99% and 98% of  $I_0$ .<sup>40</sup>

### Application of osmotic compression and expansion

To induce hypotonic/hypertonic shock ( $t = 0$  min) followed by osmotic expansion/compression, the osmolarity of the surrounding solution was altered by rapidly exchanging the imaging buffer.<sup>35</sup> For osmotic expansion, the isotonic Tyrode-HEPES buffer solution (isotonic osmolarity of  $295 \text{ mOsmol L}^{-1}$ ) pH 7.4, was rapidly exchanged with hypotonic buffer solution by diluting isotonic Tyrode-HEPES buffer with pure  $\text{H}_2\text{O}$  (HPLC quality, Fischer Chemical GmbH, Schwerte, Germany) at different volume percentages (20, 30, 40, 50, 60, or 80% pure  $\text{H}_2\text{O}$  of the final solution), resulting in decreased osmolarities (236, 206, 177, 147, 118, and  $59 \text{ mOsmol L}^{-1}$ ). For platelet compression, the isotonic Tyrode-HEPES buffer solution was rapidly exchanged with hypertonic buffer solution by mixing Tyrode-HEPES buffer with D-sorbitol (S1876-100G, Sigma Aldrich) at different concentrations (59, 118, 154, 200, 236, 267, 300, and 350 mM) resulting in increased osmolarities (354, 412, 449, 495, 531, 567, 595, and  $645 \text{ mOsmol L}^{-1}$ ) without affecting the viability of the platelet.<sup>41</sup> To achieve osmotic expansion in

MEF cells, isotonic L-15 medium ( $320 \text{ mOsmol L}^{-1}$ ) was rapidly replaced with a hypotonic medium [L-15 medium diluted with pure  $\text{H}_2\text{O}$  (HPLC quality, Fischer Chemical GmbH, Schwerte, Germany) at different volume percentages (20, 40 or 60% pure  $\text{H}_2\text{O}$  of the final solution)] which resulted in decreased osmolarity (256, 192 or  $128 \text{ mOsmol L}^{-1}$ ). To achieve osmotic expansion, the isotonic L-15 medium was also quickly replaced with hypertonic medium L-15 medium mixed with sucrose<sup>42</sup> (S0389, Sigma Aldrich, at concentrations 250, 300, and 450 mM), resulting in an overall increase in osmolarity (570, 320, and  $770 \text{ mOsmol L}^{-1}$ ).

### Spatial confinement

Spatial confinement of platelets was achieved by microcontact printing as described previously.<sup>5,28</sup> Briefly, a PDMS stamp (Sylgard 184, The Dow Chemical Company, Midland, Michigan, USA) was fabricated by mixing the polymer with crosslinker (1:10 ratio), centrifuging at  $230 \times g$  for 5 min and spreading over a custom-made line-structured silicon wafer (nominal 10- $\mu\text{m}$ -wide stripes with 5  $\mu\text{m}$  spacing resulting in 5  $\mu\text{m}$  stripes with 10  $\mu\text{m}$  spacing for the stamp<sup>28</sup>). Before baking, the wafer with PDMS was placed for 30 min under vacuum in a desiccator to further remove incorporated air bubbles. After baking at  $80 \text{ }^\circ\text{C}$  for 2 h, the PDMS stamp was slowly removed and placed for storage in a container with the structured side facing up. For the following microcontact printing, small squares were cut with a scalpel, washed with ethanol, dried with  $\text{N}_2$  gas, and then treated with oxygen plasma (Zepto-QRS 200, Diener electronics GmbH, Ebhausen, Germany) at 100% power for 30 s at  $\text{O}_2$  flow of  $0.2 \text{ mL min}^{-1}$ . The oxygen-plasma-activated PDMS stamps were then incubated for 30 min at  $37 \text{ }^\circ\text{C}$  with  $1.5 \text{ mg mL}^{-1}$  fluorescein-labeled fibrinogen (Alexa Fluor 594 Conjugate, Thermo Fisher Scientific) in PBS solution. To reduce evaporation, the PDMS stamps were covered with pieces of Parafilm (Bemis Company Inc., Neenah, USA). The incubated stamps were washed with  $\text{H}_2\text{O}$  (HPLC quality, Fischer Chemical



GmbH, Schwerte, Germany) and carefully dried with N<sub>2</sub> gas. The printing procedure was carried out using oxygen-plasma-activated (100% power, 30 s, O<sub>2</sub> flow 0.2 mL min<sup>-1</sup>) glass-bottom cell culture dish (81158,  $\mu$ -dish glass bottom, ibidi GmbH, Gräfelfing, Germany). The fibrinogen-coated PDMS stamps were carefully placed on the glass with the fibrinogen/structured side facing the glass and incubated for another 15 min at 37 °C. After removing the PDMS stamps and washing with H<sub>2</sub>O the fibrinogen structures remained on the glass of the cell culture dish. The width of the printed lines was about 3  $\mu$ m, slightly smaller as expected from the dimensions of the silicon wafer due to inaccuracies in the fabrication process.<sup>28</sup> The dish could be stored for at least one week with 1 mL H<sub>2</sub>O in an incubator at 37 °C. To passivate the areas without fibrinogen coating, the cell culture dishes were incubated for 1 h at 37 °C with a mixture of 10 mM HEPES in PBS and 5.7  $\mu$ g mL<sup>-1</sup> PLL-PEG (PLL (20 kDa) grafted with PEG (2 kDa), SuSoS AG, Dübendorf, Switzerland) and washed three times with H<sub>2</sub>O.

### SICM data analysis

Topography and stiffness data were analyzed and processed using Igor Pro 9 (WaveMetrics, Inc., Portland, Oregon, USA). To calculate platelet area  $A$  and volume  $V$ , all height images were corrected for  $z$ -offset and tilt using a first-order line flattening. Platelets were identified by applying a pixel height threshold of  $h = 50$  nm, where all pixels below were considered as substrate. Area  $A$  of each platelet was calculated using the formula  $A = \sum_i a_i$ , where  $a_i$  represents the area of each pixel corresponding to the platelet. Volume  $V$  was calculated using the formula  $V = A \times \bar{h}$ , where area  $A$  is multiplied with the mean height  $\bar{h}$ . This is mathematically equivalent to summing the volumes of all pixels corresponding to the platelet.<sup>31</sup>

As the finite thickness of the platelets affects the stiffness measured by SICM, the Young's modulus data (except for Fig. S1A and B, indicated by uncorrected) was corrected for the finite thickness of the platelets using a correction model published earlier.<sup>43</sup> The platelet stiffness was quantified as the median of the corrected Young's modulus  $E$  for each platelet. Although the absolute stiffness values are slightly higher overall without applying this correction, the relative stiffness changes remain similar (Fig. S1), proving that SICM robustly measures volume-induced stiffness changes.

For all time-resolved measurements, platelets were imaged during induced hypotonic/hypertonic shock to achieve osmotic expansion/compression (see above), which was the time point defined as  $t = 0$  min. To increase measurement throughput, some platelets were imaged with SICM only once before ( $t \approx -1$  min) and directly after ( $t \approx 1-2$  min) hypotonic/hypertonic shock. The initial volume  $V_0$  represents the platelet volume right before hypotonic/hypertonic shock. The relative volume  $\nu$  was then calculated as  $\nu = V/V_0$  with the initial volume  $V_0$ .

For spreading platelets, relative area  $a$  and relative volume  $\nu$  of the spread platelets were calculated as follows:  $a = A/A_{\text{final}}$  and  $\nu = V/V_{\text{final}}$  with  $A_{\text{final}}$  and  $V_{\text{final}}$  as the final spread area and the final volume after  $t = 20$  min, respectively.

The bar plots in Fig. 5 and Fig. S6B are represent as median values with error bars denoting the standard error of the median calculated as  $1.48 \text{ MAD}/\sqrt{N}$  with median absolute deviation (MAD).<sup>44</sup>

As the platelet stiffness values typically follows a log-normal distribution,<sup>26</sup> fitting was performed on logarithmic  $E$  values.

### Statistical analysis

Igor Pro 9 (WaveMetrics, Inc., Portland, Oregon, USA) was used for all statistical tests. For comparison between two groups, an unpaired two-tailed  $t$ -test was used. For more than two groups, a Tukey's range test was used. The results were considered to be significantly different for  $P \leq 0.05$  (\*),  $P \leq 0.01$  (\*\*), and  $P \leq 0.001$  (\*\*\*) or not significant (ns) for  $P > 0.05$ . For each treatment, platelets from 3 to 6 different donors were used in independent experiments.

## Results and discussion

### Platelet stiffness changes during osmotic expansion and compression

Topography and mechanical stiffness of human platelets were investigated with SICM (Fig. 1A). Initially, single platelets were imaged in an isotonic Tyrode-HEPES buffer. To induce an osmotic shock, the isotonic buffer was subsequently replaced with either a hypotonic or a hypertonic buffer, thereby increasing or decreasing osmolarity, triggering osmotic expansion or compression, respectively.<sup>45-49</sup> For an increasing osmolarity, the platelet height increased due to osmotic expansion resulting from a water influx into the platelet due to osmotic pressure (Fig. 1B, topography images). Importantly, this osmotic expansion was accompanied by a decrease in platelet stiffness (Fig. 1B, stiffness image). In contrast, an overall decrease in platelet height and stiffening of the platelet was observed for osmotic compression due to osmolarity increase (Fig. 1C).

As platelets can exhibit volume regulation after osmotic change,<sup>41,49,50</sup> we speculated that this is accompanied by a time-dependent change in platelet stiffness. Therefore, we investigated the time-dependent relationship between volume and stiffness of individual living platelets using SICM<sup>26,35</sup> by continuously imaging platelets over time during osmotic expanding and compression (Fig. 2). For platelets during osmotic expansion (Fig. 2A), the platelet volume  $V$  rapidly increased within 1 min after hypotonic shock and then slowly decreased (Fig. 2A, right, black trace). This volume decrease after hypotonic shock is commonly known as regulatory volume decrease (RVD), which can occur in different cell types.<sup>41,49-52</sup> On the contrary, the platelet stiffness  $E$  rapidly decreased and then slowly increased (Fig. 2A, right, yellow trace) during the volume change. For platelets during osmotic compression (Fig. 2B), the platelet volume rapidly decreased (Fig. 2B, right, black trace) while the stiffness increased (Fig. 2B, right, yellow trace). This behavior could be observed throughout all measured platelets over time and implies that water efflux or influx leads to a decrease or increase in intracellular molecular



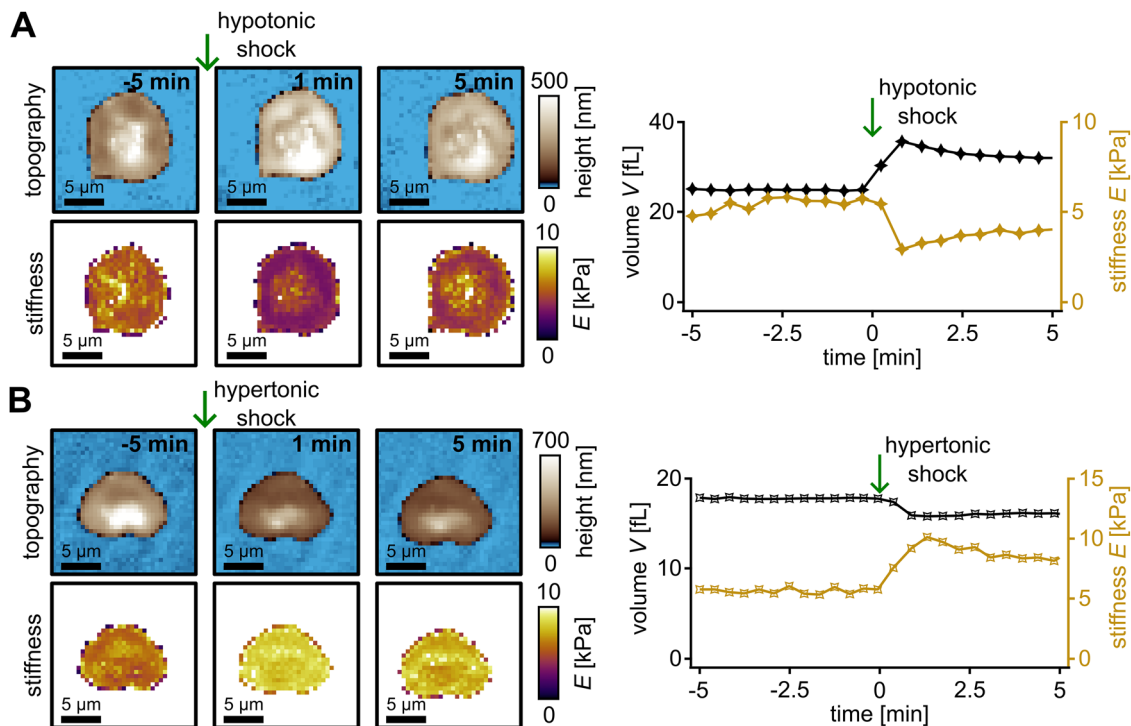


Fig. 2 Topography and stiffness images (left) and time-resolved volume and stiffness measurements (right) of platelets under (A) osmotic expansion and (B) osmotic compression induced by hypotonic and hypertonic shock, respectively. Left panels show topography and stiffness images before ( $t = -5$  min), during ( $t = 1$  min), and after ( $t = 5$  min) the hypotonic shock ((A), osmolarity:  $177 \text{ mOsmol L}^{-1}$ ) and the hypertonic shock ((B), osmolarity:  $354 \text{ mOsmol L}^{-1}$ ), respectively. Right panels show measured volume  $V$  and corresponding stiffness  $E$  over time with the hypotonic (A) and the hypertonic shock (B) at  $t = 0$  min.

crowding,<sup>15,18</sup> which could also directly impact the mechanical properties of platelets, potentially also through modulation of cytoskeleton tension<sup>53</sup> or volumetric constraints.<sup>54</sup>

### Platelet stiffness correlates inversely with platelet volume change

While absolute initial platelet volume  $V_0$  and platelet stiffness  $E$  in isotonic buffer were generally not correlated but randomly distributed, here between 1 to 10 kPa and between 4 to 34 fL, respectively (Fig. S2A), the relationship between platelet volume  $V$  and stiffness  $E$  depicted in the time-resolved data (Fig. 2) indicates that for individual platelets there might be an inverse correlation between these two parameters during osmotic expansion and compression. This led us to the hypothesis that platelet stiffness is directly correlated with platelet volume, as reported earlier for several other types of mammalian cell.<sup>14,15,37</sup>

When considering the platelet during osmotic compression (Fig. 2B), stiffness and absolute volume  $V$  were indeed strongly correlated (Fig. 3A, platelet 1) and followed the correlation (Fig. 3A, left red curve) described earlier for other cell types<sup>14,15</sup> quantified as

$$E(V) = X \frac{V}{(V - V_{\min})^2}. \quad (1)$$

$V_{\min}$  is the absolute minimum cell volume following maximum compression and  $X$  is a constant related to the cell stiffness and governed by the osmotic pressure inside the cell.<sup>14,15</sup> For

individual platelets, we here found values for  $V_{\min}$  of a few fL's and values for  $X$  on the order of 10 kPa fL.

When considering the platelet during osmotic expansion (Fig. 2A), volume and stiffness also followed a similar correlation (Fig. 3A, platelet 2, right red curve), however, shifted laterally due to the difference in absolute volume as platelets have, by nature, a large spread in volume<sup>35,55</sup> (Fig. S2A).

We therefore calculated the relative volume  $v = V/V_0$  and when plotting the stiffness  $E$  vs. the relative volume  $v$  the two platelets during osmotic compression/expansion indeed roughly followed the same correlation (Fig. 3A, inset). Normalizing eqn (1) to the relative volume gives

$$E(v) = x \frac{v}{(v - v_{\min})^2} \quad (2)$$

with the relative minimum volume  $v_{\min} \cong V_{\min}/V_0$  and stiffness scaling factor  $x \cong X/V_0$ , which now well described both platelets (Fig. 3A, inset, blue curve) giving  $v_{\min} \approx 0.4$  and  $x \approx 2$  kPa for these two platelets. For higher accuracy, we then considered many different platelets at different osmotic conditions (Fig. 3B). Fitting eqn (2) to the stiffness vs. relative volume data of many platelets (Fig. 3B, blue curve) gives a relative minimum volume of  $v_{\min} = 0.57 \pm 0.01$  and  $x = 1.3 \pm 0.2$  kPa.

The minimum volumes,  $V_{\min}$  and  $v_{\min}$ , are directly related to the non-soluble, non-osmotic volume and volume fraction of cells, respectively, representing the incompressible portion of cellular volume that remains constant under osmotic stress.<sup>14</sup> A non-osmotic fraction of 0.3–0.5 is typically reported for



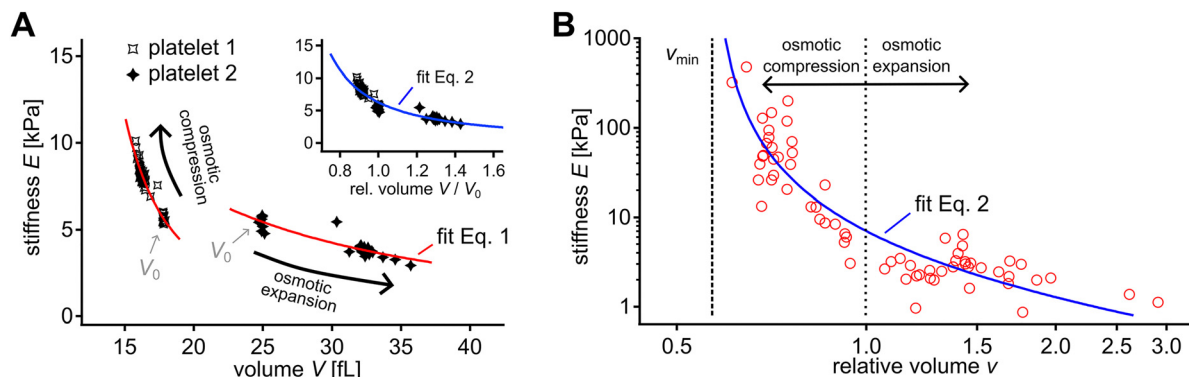


**Fig. 3** Correlation between platelet volume and stiffness. (A) Stiffness  $E$  vs. volume  $V$  during osmotic expansion/compression from time-dependent measurements of the two platelets shown in Fig. 2A and B, respectively, with individual fits of eqn (1) (red curves). The inset shows stiffness  $E$  vs. relative volume  $V/V_0$  for the two platelets with common fit of eqn (2) (blue curve). (B) Stiffness  $E$  values vs. relative volume  $v = V/V_0$  of multiple platelets after osmotic compression/expansion. Fitting eqn (2) (blue curve) gives a relative minimum volume  $v_{\min} = 0.57 \pm 0.01$  (black dashed line). Number of platelets:  $n = 68$  from 5 different donors at 14 different osmotic conditions in 10 independent experiments.

platelets,<sup>35,41,48–50,52,56</sup> and other cells,<sup>57–59</sup> which is within the range of the values of relative minimum volume of 0.2 to 0.5 found here.

As platelet adhesion to the cellular or extracellular matrix components is a central aspect of their function,<sup>60</sup> we also investigated the behavior of platelets adhered to matrix proteins (Fig. S3). Platelets adhered to fibrinogen-coated surfaces (Fig. S3A and B) showed the same softening and stiffening behavior upon osmotic expansion and compression, respectively, as previously shown (see Fig. 2). Moreover, during this expansion and compression, platelets adhered to fibrinogen-coated surfaces exhibited the same inverse correlation between stiffness and volume (Fig. S3C) as platelets on cell culture dishes (Fig. S3C, blue curve, from Fig. 3B).

Additionally, platelets are also known to interact with adjacent cells, for example, by formation of gap junctions *via* connexins.<sup>61</sup> We hence also examined if the contact of adjacent platelets affects the observed inverse correlation between volume and stiffness (Fig. S4). Two platelets in contact with each other showed the expected softening and stiffening behavior upon osmotic expansion and compression, respectively (Fig. S4A and B). Moreover, the platelets in contact also exhibited the same inverse correlation between stiffness and volume (Fig. S4C) as single platelets (Fig. S4C, blue curve, from Fig. 3B).

We found a similar inverse correlation between volume and stiffness of osmotically compressed fibroblast cells (Fig. S5) as reported in earlier studies,<sup>14,15</sup> which demonstrates the reliability of SICM in probing both cell volume and stiffness at the single cell level. Interestingly, fibroblast cells softening upon osmotic expansion also followed the same stiffness *vs.* volume correlation as for compression (Fig. S5, blue curve), indicating the importance of this behavior.

### The inverse stiffness *vs.* volume correlation is also present with an inhibited actin cytoskeleton

Next, we investigated the influence of the actin cytoskeleton on the inverse volume-stiffness correlation. Adherent platelets have a polymerized actin cytoskeleton, which influences platelets

morphology and function.<sup>12,62</sup> We performed time-resolved SICM imaging of adherent platelets with an inhibited actin cytoskeleton using cytochalasin D (cytoD) under osmotic compression and expansion (Fig. S6A, left). Ten minutes before the hypotonic/hypertonic shock, we added cytoD and viewed its depolymerization effect on the cytoskeleton with a decrease in stiffness  $E$  but no change in volume (Fig. S6A, right). At  $t = 0$  min, we induced a hypotonic or hypertonic shock (Fig. S6A, right) to achieve osmotic expansion or compression (to 177 mOsmol L<sup>-1</sup> and 412 mOsmol L<sup>-1</sup>, respectively). As for untreated platelets, the volume and stiffness of cytoD-treated platelets either increased and decreased (osmotic expansion) or decreased and increased (osmotic compression), respectively (Fig. S6A and S7).

On average, we found no significant volume change after adding cytoD (Fig. S6B, left,  $P = 0.64$ ), but a significant decrease in stiffness  $E$  after treatment with cytoD (Fig. S6B, right,  $P = 0.0043$ ), consistent with the literature.<sup>26</sup> For osmotic compression or expansion of cytoD-treated platelets, the previously observed behavior of an increase/decrease in relative volume  $v$  (Fig. S6B, left,  $P = 9.6 \times 10^{-6}$  and  $P = 5.3 \times 10^{-9}$ ) accompanied by a decrease or increase, respectively, in the average stiffness (Fig. S6B, right,  $P = 9.5 \times 10^{-12}$  and  $P = 0.011$ ) was still prominent even though actin cytoskeleton polymerization was inhibited by cytoD. Plotting stiffness *vs.* relative volume for the cytoD-treated and then osmotically expanded/compressed platelets (Fig. S6C, filled markers) shows a similar relationship to that observed for normal (untreated) platelets (Fig. S6C, open markers). While the exact values differ, the general pattern of the inverse correlation between stiffness and volume remains consistent in both groups. Fitting eqn (2) to the cytoD-treated platelet data yields  $v_{\min} = 0.49 \pm 0.02$  and  $x = 1.0 \pm 0.1$  kPa (Fig. S6C, dashed blue curve). Hence, the inverse correlation curve is similar but shifted downwards towards lower stiffness, as shown by the lower  $x$  value compared to the normal (untreated) platelets ( $x = 1.3 \pm 0.1$  kPa, from Fig. 3B).

This demonstrates that cytoD has a softening effect and conversely that the actin cytoskeleton contributes to platelet stiffness,<sup>22,63</sup> in addition to the effect of the osmotic



compression or expansion, as the inverse correlation is still present even without an intact actin cytoskeleton.<sup>14,15</sup>

### Spreading platelets follow the inverse stiffness vs. volume correlation

We then investigated whether the inverse correlation between stiffness  $E$  and platelet volume  $V$  observed in our initial measurements is also generally present in further physiologically important processes and investigated platelets dynamically spreading on a flat surface (Fig. 4). Platelets undergo a shape change from the resting state in solution (discoid or spherical shape) to an adherent state (spread-out, flattened shape).<sup>64,65</sup> A previous SICM study showed that the stiffness of spreading platelets increased over time.<sup>26</sup> Hence, we observed the area  $A$ , the volume  $V$ , and the stiffness  $E$  of spreading platelets with SICM in order to determine if the relation between volume and stiffness is also present for spreading platelets.

Benefitting from the high time resolution in our SICM experiments, we imaged platelets during spreading on a substrate (Fig. 4A, top), where they showed the hypothesized behavior that the increase in spreading area is accompanied by a decrease in volume (Fig. 4B) and an increase in stiffness over time (Fig. 4A, bottom, and Fig. S8). Plotting stiffness vs. volume shows that spreading platelets indeed follow an inverse correlation (Fig. 4C), the same inverse correlation as for osmotic compression/expansion (Fig. 4C, blue curve, from Fig. 3B).

To investigate whether platelets also show the inverse correlation between stiffness and volume during the spreading process, we prepared platelets on non-coated cell culture dishes to prevent the platelets from spreading (Fig. S9). Non-spread platelets also showed the expected softening and stiffening

behavior upon osmotic expansion and compression, respectively (Fig. S9A and B). Moreover, non-spread platelets also exhibited an inverse correlation between stiffness and volume (Fig. S9C), but with stiffness slightly shifted towards lower values compared to spread platelets, which is consistent with the observation that platelets are generally softer when not fully spread (see Fig. 4).

The increase in stiffness during spreading was also found for other cell types<sup>15</sup> and can probably be attributed to cytoskeleton reorganization in the platelets, particularly actin polymerization and microtubule dynamics, which generate contractile forces and stabilize the spread-out morphology.<sup>63,66</sup> This cytoskeleton adjustment is essential for platelets to effectively perform their hemostatic functions.<sup>67</sup> These results of dynamically spreading platelets supported our hypothesis that the observed inverse correlation between volume and stiffness appears to be a general characteristic of living platelets.

### Spatially confined platelets follow the inverse stiffness vs. volume correlation

As a further physiologically relevant situation, we investigated whether spatial confinement affects platelet volume  $V$  and stiffness  $E$ , and whether the relationship between these parameters aligns with the general correlation observed in unconfined platelets. We used microcontact printing to confine platelets to 3  $\mu\text{m}$  wide fibrinogen lines (Fig. 5A and Fig. S10). The quality of the fibrinogen lines was determined by epifluorescence using fluorescein-labeled fibrinogen (Fig. S10, left panels). Absolute volume  $V$  and stiffness  $E$  of unconfined and spatially confined platelets were determined with SICM showing significantly ( $P = 0.023$ ) higher volumes  $V$  (Fig. 5B, left) and significantly

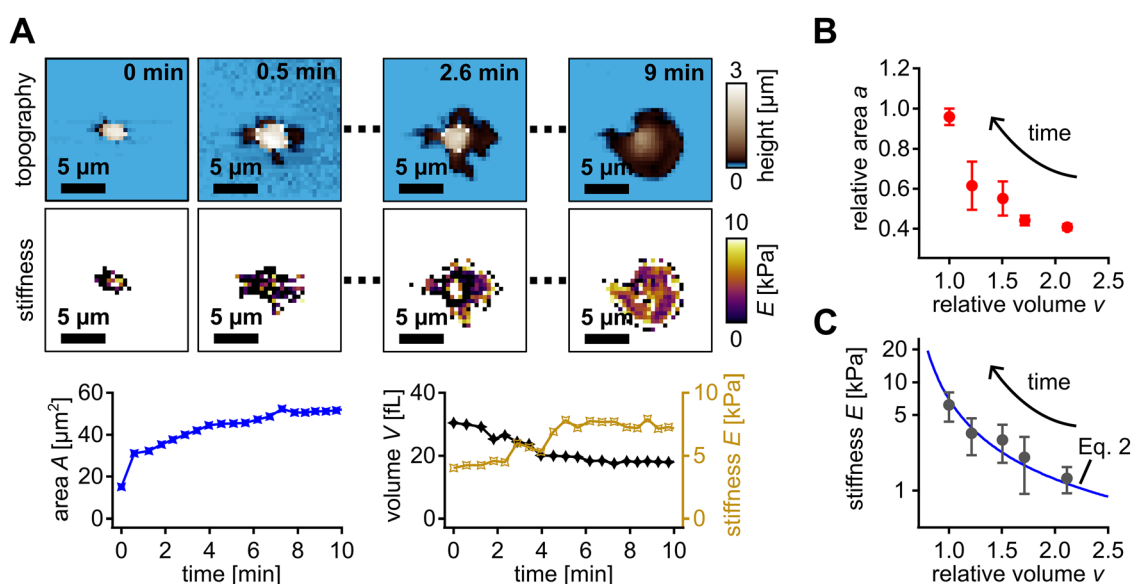


Fig. 4 Area, volume, and stiffness measurements of dynamically spreading platelets. (A, top) Topography with corresponding stiffness images of a spreading platelet at different time points. (A, bottom) Corresponding area, volume, and stiffness vs. time curves of the platelet shown above. Averaged time graphs of all measured spreading platelets can be found in Supplement Information (Fig. S7). (B) Platelet relative area  $a$  and (C) stiffness  $E$  vs. relative volume  $v$  (median values  $\pm$  MAD of platelets binned in intervals of 0.25 relative volume), with the inverse correlation from Fig. 3B (blue curve). Number of platelets:  $n = 20$  from 3 different donors in 3 independent experiments.



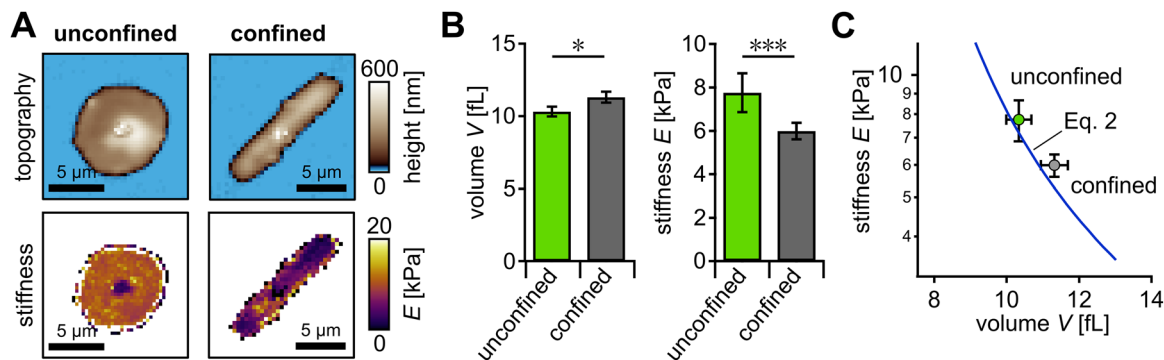


Fig. 5 SICM measurements of spatially confined platelets. (A) Representative topography (top) and stiffness (bottom) images of unconfined (left) and confined (right) platelets. (B) Comparison between median platelet volume  $V$  (left) and median platelet stiffness  $E$  (right) of unconfined (green) and confined platelets (grey). (C) Stiffness vs. volume data for unconfined (green) and confined (grey) platelets with the prediction of the inverse correlation (red line) from eqn (2) (from Fig. 3B, using  $V_0 = 10.4$  fL for unconfined platelets). Number of platelets:  $n$  (unconfined) = 151,  $n$  (confined) = 251 from 3 different donors in 4 independent experiments.

( $P = 1.3 \times 10^{-5}$ ) lower stiffness  $E$  (Fig. 5B, right) of confined platelets compared to unconfined platelets. This indicates that volume  $V$  and stiffness  $E$  of unconfined and confined platelets are again consistent with the inverse correlation (Fig. 5C) from osmotic compression/expansion (Fig. 5C, blue curve, from Fig. 3B, inset).

An inverse correlation between volume and stiffness for different spatial confinement was also found for other cell types.<sup>15</sup> Spatially confined platelets, which have only rarely been investigated so far, offer a deeper understanding of platelet morphology in different shapes, environments, and situations.

## Conclusion

We investigated the relation of volume and stiffness of single, adhered human platelets using SICM with submicrometer spatial resolution (Fig. 1). As a non-contact technique, SICM is beneficial in comparison to other nanoindentation techniques such as atomic force microscopy (AFM), which are often challenging due to the risk of unwanted platelet activation by direct mechanical contact.<sup>68</sup> Mechanical activation would not only alter the mechanical properties of the platelets, but is also associated with a reduction in their viability due to activation-induced morphological and functional changes.<sup>69</sup> Platelet activation during the washing, preparation, or adhesion might also influence platelet function.<sup>70</sup> However, as adherent cells are generally required for both AFM and SICM, other techniques such as micropipette aspiration or real-time deformability cytometry would be needed to investigate the osmotic behavior of non-adherent platelets.<sup>36</sup>

By osmotic expansion/compression, we measured volume and stiffness of individual platelets (Fig. 1B and C). We demonstrated that platelets exhibit both short-term (within  $\sim 1$  minute) and long-term (within  $\sim 2$ –5 minutes, during volume regulation) changes in volume and stiffness after osmotic expansion/compression (Fig. 2). On both short- and long-term time scales, with decreasing (increasing) osmolarity of the surrounding medium, the platelets showed a volume increase (decrease), with a decrease

(increase) in platelet stiffness (Fig. 3A). Therefore, we measured platelets at several different osmolarities and found an inverse correlation between volume and stiffness during osmotic expansion/compression (Fig. 3B). A similar correlation was previously found for different eukaryotic cells<sup>15</sup> and for fibroblasts (Fig. S5). While, to our knowledge, only osmotic compression has been investigated in the literature,<sup>14,15</sup> we here show that platelets and fibroblasts exhibit the same respective inverse volume-stiffness correlation for both osmotic expansion and compression, underlining the importance of this relationship.

Furthermore, cytoD-treated platelets under osmotic compression/expansion were shown to exhibit a similar stiffness vs. volume correlation as untreated platelets (Fig. S6 and S7). As expected, the effect of actin depolymerization by cytoD showed a significant decrease in platelet stiffness, as SICM is known to probe the platelet cytoskeleton.<sup>12</sup> However, the inverse stiffness vs. volume correlation curve was slightly shifted downwards compared to the correlation curve without cytoD treatment, showing that the actin cytoskeleton contributes to platelet stiffness in addition to the osmotic compression/expansion. Nevertheless, the interpretation of the observed inverse stiffness vs. volume correlation and its physical origin and the influence of the cell cortex are still not entirely clear.<sup>15</sup> As the cell cytoskeleton is too weak to withstand osmotic pressure, the cell probably “feels” the osmotic shock *via* the change in cortex tension<sup>71</sup> and then responds due to the contractile tension by active water transport, for example, *via* ion channels, and thereby alter the molecular crowding in the cytoplasm.<sup>14,15,18</sup> The molecular crowding also influences cell viscoelasticity,<sup>72</sup> which is also probed by SICM.<sup>73</sup> An additional contribution on cell stiffness might result from cell membrane folding and tension, which were found to be also affected by cell osmosis.<sup>74–76</sup>

We then investigated two further physiologically relevant processes: spreading platelets and spatially confined platelets. Platelets are unique as they undergo a programmed shape change (from spherical to spread out) when they adhere to a substrate. As was previously known for other cells,<sup>15</sup> we showed that platelet spreading is accompanied with a decrease in



volume and an increase in stiffness (Fig. 4A), thereby effectively “moving up” on the inverse stiffness vs. volume correlation (Fig. 4C). Spatially confined platelets have rarely been investigated so far. Here, we determined the influence of confinement on platelet morphology and stiffness with the aid of microcontact printing (Fig. 5A). Line-confined platelets were significantly larger in volume and significantly smaller in stiffness compared to unconfined platelets (Fig. 5B), consistent with the observed inverse volume-stiffness relationship (Fig. 5C). In conclusion, platelets appear to follow the inverse stiffness vs. volume correlation also in physiologically relevant situations.

Interestingly, platelet stiffness does not appear to be correlated with the (initial) absolute volume in spread platelets (Fig. S2A) or with the spreading area (Fig. S2B). While the reason for this is unclear, a possible explanation could be that, during adhesion, platelets spread and thereby stiffen (see Fig. 4) until they reach a possibly predefined stiffness, which might be related to molecular crowding, biomolecular condensates, or membrane folding or tension in the platelet.<sup>75,76</sup>

To summarize this work, we used SICM to determine the correlation between platelet volume and stiffness during osmotic compression/expansion, during platelet spreading, as well as under spatial confinement. By finding this general correlation between platelet volume and stiffness, we might provide new insights into how platelets maintain their structural integrity<sup>77</sup> and respond to their environment,<sup>6,53,78</sup> which is fundamental to numerous biological processes.<sup>79</sup> As volumetric compression is a ubiquitous phenomenon in the human body, for example, during development, movement, digestion, and tumorigenesis but also injury,<sup>76</sup> our findings also provide insights into the mechanical properties of platelets and their potential role in various physiological and pathological processes.<sup>6,13,53</sup> The consistency of this correlation across different experimental conditions underscores its fundamental nature for platelets, similar as for many other cell types.<sup>76</sup> One important implication is that platelet volume and stiffness are not independent of each other, hence in situations where the platelet volume changes, the platelet stiffness also changes.<sup>13</sup> Future research could explore the impact of this volume-stiffness relationship on platelet function in thrombosis and hemostasis,<sup>80</sup> how alterations in this correlation contribute to platelet-related disorders,<sup>81</sup> the potential use of platelet mechanical properties as biomarkers for cardiovascular diseases,<sup>82</sup> and the development of novel therapeutic approaches targeting platelet mechanics.<sup>83</sup> Understanding these interactions in platelets not only enriches our comprehension of platelet biomechanics but also opens up new ways for diagnostic and therapeutic strategies to manage conditions where platelet function is impaired.

## Author contributions

KK, JR, JS, MG, and TS designed the study. KK and JR performed the experiments and analyzed data. All authors interpreted data, discussed results, drafted and revised the manuscript.

## Conflicts of interest

The authors declare no conflicts of interest.

## Data availability

The data supporting this article have been included in the supplementary information (SI) or will be made available upon request.

Supplementary information (SI) is available. See DOI: <https://doi.org/10.1039/d5sm00839e>.

## Acknowledgements

This work was funded by the Deutsche Forschungsgemeinschaft (DFG, German Research Foundation) - Projektnummer 335549539/GRK2381 and Projektnummer 374031971-TRR 240. We thank Vincent Gidlund for the training in microcontact printing and providing the wafer.

## References

- 1 A. T. Nurden, *Thromb. Haemostasis*, 2011, **105**(S 06), S13–33.
- 2 M. R. Thomas and R. F. Storey, *Thromb. Haemostasis*, 2015, **114**(03), 449–458.
- 3 A. Scridon, *Int. J. Mol. Sci.*, 2022, **23**, 12772.
- 4 A.-K. Rohlfing, K. Kolb, M. Sigle, M. Ziegler, A. Bild, P. Münzer, J. Sudmann, V. Dicenta, T. Harm, M.-C. Manke, S. Geue, M. Kremser, M. Chatterjee, C. Liang, H. von Eysmond, T. Dandekar, D. Heinzmann, M. Günter, S. von Ungern-Sternberg, M. Büttcher, T. Castor, S. Mencl, F. Langhauser, K. Sies, D. Ashour, M. C. Beker, M. Lämmerhofer, S. E. Autenrieth, T. E. Schäffer, S. Laufer, P. Szklanna, P. Maguire, M. Heikenwalder, K. A. L. Müller, D. M. Hermann, E. Kilic, R. Stumm, G. Ramos, C. Kleinschnitz, O. Borst, H. F. Langer, D. Rath and M. Gawaz, *Nat. Commun.*, 2022, **13**, 1823.
- 5 A. Kita, Y. Sakurai, D. R. Myers, R. Rounsevell, J. N. Huang, T. J. Seok, K. Yu, M. C. Wu, D. A. Fletcher and W. A. Lam, *PLoS One*, 2011, **6**, e26437.
- 6 M. F. Kee, D. R. Myers, Y. Sakurai, W. A. Lam and Y. Qiu, *PLoS One*, 2015, **10**, e0126624.
- 7 J. G. White, E. L. Leistikow and G. Escolar, *Blood Cells*, 1990, **16**, 43–70.
- 8 S. Vogel, R. Bodenstern, Q. Chen, S. Feil, R. Feil, J. Rheinlaender, T. E. Schäffer, E. Bohn, J.-S. Frick, O. Borst, P. Münzer, B. Walker, J. Markel, G. Csanyi, P. J. Pagano, P. Loughran, M. E. Jessup, S. C. Watkins, G. C. Bullock, J. L. Sperry, B. S. Zuckerbraun, T. R. Billiar, M. T. Lotze, M. Gawaz and M. D. Neal, *J. Clin. Invest.*, 2015, **125**, 4638–4654.
- 9 M. Holinstat, *Cancer Metastasis Rev.*, 2017, **36**, 195–198.
- 10 J. E. Italiano Jr, W. Bergmeier, S. Tiwari, H. Falet, J. H. Hartwig, K. M. Hoffmeister, P. André, D. D. Wagner and R. A. Shivdasani, *Blood*, 2003, **101**, 4789–4796.
- 11 J. H. Hartwig, *Semin. Hematol.*, 2006, **43**, S94–100.



- 12 C. Zaninetti, L. Sachs and R. Palankar, *Hamostaseologie*, 2020, **40**, 337–347.
- 13 O. Oshinowo, S. S. Azer, J. Lin and W. A. Lam, *J. Thromb. Haemostasis*, 2023, **21**, 2339–2353.
- 14 E. H. Zhou, X. Trepapat, C. Y. Park, G. Lenormand, M. N. Oliver, S. M. Mijailovich, C. Hardin, D. A. Weitz, J. P. Butler and J. J. Fredberg, *Proc. Natl. Acad. Sci. U. S. A.*, 2009, **106**, 10632–10637.
- 15 M. Guo, A. F. Pegoraro, A. Mao, E. H. Zhou, P. R. Arany, Y. Han, D. T. Burnette, M. H. Jensen, K. E. Kasza, J. R. Moore, F. C. Mackintosh, J. J. Fredberg, D. J. Mooney, J. Lippincott-Schwartz and D. A. Weitz, *Proc. Natl. Acad. Sci. U. S. A.*, 2017, **114**, e8618–e8627.
- 16 D. Oh, A. Zidovska, Y. Xu and D. J. Needleman, *Biophys. J.*, 2011, **101**, 1546–1554.
- 17 J. Irianto, J. Swift, R. P. Martins, G. D. McPhail, M. M. Knight, D. E. Discher and D. A. Lee, *Biophys. J.*, 2013, **104**, 759–769.
- 18 Y. Li, M. Chen, J. Hu, R. Sheng, Q. Lin, X. He and M. Guo, *Cell Stem Cell*, 2021, **28**, 63–78.e67.
- 19 S. Suresh, *Acta Biomater.*, 2007, **3**, 413–438.
- 20 H. Jiang and S. X. Sun, *Biophys. J.*, 2013, **105**, 609–619.
- 21 F. J. Byfield, R. K. Reen, T. P. Shentu, I. Levitan and K. J. Gooch, *J. Biomech.*, 2009, **42**, 1114–1119.
- 22 D. A. Fletcher and R. D. Mullins, *Nature*, 2010, **463**, 485–492.
- 23 V. Swaminathan, K. Myhreye, E. T. O'Brien, A. Berchuck, G. C. Blobe and R. Superfine, *Cancer Res.*, 2011, **71**, 5075–5080.
- 24 G. Davi and C. Patrono, *N. Engl. J. Med.*, 2007, **357**, 2482–2494.
- 25 J. E. Aslan, A. Itakura, J. M. Gertz and O. J. McCarty, *Methods Mol. Biol.*, 2012, **788**, 91–100.
- 26 J. Rheinlaender, S. Vogel, J. Seifert, M. Schächtele, O. Borst, F. Lang, M. Gawaz and T. E. Schäffer, *Thromb. Haemostasis*, 2015, **113**, 305–311.
- 27 J. Seifert, J. Rheinlaender, H. von Eysmond and T. E. Schäffer, *Nanoscale*, 2022, **14**, 8192–8199.
- 28 J. G. Rodríguez, J. Seifert, V. Gidlund, C. Rianna and T. E. Schäffer, *Biophys. Rep.*, 2025, 100222.
- 29 H. Yan, C. Naadiya, W. Yiming, C. Reid, M. Alexandra and N. Heyu, *J. Biomed. Res.*, 2015, **29**, 437–444.
- 30 P. K. Hansma, B. Drake, O. Marti, S. A. Gould and C. B. Prater, *Science*, 1989, **243**, 641–643.
- 31 Y. E. Korchev, J. Gorelik, M. J. Lab, E. V. Sviderskaya, C. L. Johnston, C. R. Coombes, I. Vodnyanoy and C. R. Edwards, *Biophys. J.*, 2000, **78**, 451–457.
- 32 X. Liu, Y. Li, H. Zhu, Z. Zhao, Y. Zhou, A.-M. Zaske, L. Liu, M. Li, H. Lu, W. Liu, J.-F. Dong, J. Zhang and Y. Zhang, *Platelets*, 2015, **26**, 480–485.
- 33 Y. Zhang, X. Liu, L. Liu, A. M. Zaske, Z. Zhou, Y. Fu, X. Yang, J. L. Conyers, M. Li, J. F. Dong and J. Zhang, *Thromb. Haemostasis*, 2013, **110**, 331–339.
- 34 J. A. Nестele, A.-K. Rohlffing, V. Dicenta, A. Bild, D. Eiffler, F. Emschermann, M. Kremser, K. Krutzke, T. E. Schäffer, O. Borst, M. Levi, N. Korin and M. P. Gawaz, *Int. J. Mol. Sci.*, 2022, **23**, 11.
- 35 K. Krutzke, J. Seifert, M. Gawaz, J. Rheinlaender and T. E. Schäffer, *Thromb. Haemostasis*, 2025, **125**, 340–351.
- 36 L. Sachs, C. Denker, A. Greinacher and R. Palankar, *Res. Pract. Thromb. Haemostasis*, 2020, **4**, 386–401.
- 37 H.-S. Liao, P. J. Wen, L.-G. Wu and A. J. Jin, *J. Biomech. Eng.*, 2018, **140**, 054502.
- 38 Z. Laspa, A.-K. Rohlffing and M. P. Gawaz, *J. Visualized Exp.*, 2025, **220**, e67878.
- 39 J. Rheinlaender and T. E. Schäffer, *Anal. Chem.*, 2015, **87**, 7117–7124.
- 40 J. Rheinlaender and T. E. Schäffer, *Soft Matter*, 2013, **9**, 3230–3236.
- 41 F. Lang, *J. Am. Coll. Nutr.*, 2007, **26**, 613s–623s.
- 42 R. Alfieri, P. G. Petronini, S. Urbani and A. F. Borghetti, *Biochem. J.*, 1996, **319**(Pt 2), 601–606.
- 43 J. Rheinlaender and T. E. Schäffer, *Appl. Phys. Lett.*, 2020, **117**, 113701.
- 44 P. J. Rousseeuw and C. Croux, *J. Am. Stat. Assoc.*, 1993, **88**, 1273–1283.
- 45 B. K. Kim and M. G. Baldini, *Transfusion*, 1974, **14**, 130–138.
- 46 M. H. Summerer, P. V. Genco and A. J. Katz, *Ann. Clin. Lab. Sci.*, 1978, **8**, 447–452.
- 47 E. Watanabe and S. Sasakawa, *Thromb. Res.*, 1983, **31**, 13–21.
- 48 W. J. Armitage, N. Parmar and C. J. Hunt, *J. Cell. Physiol.*, 1985, **123**, 241–248.
- 49 A. Livne, S. Grinstein and A. Rothstein, *J. Cell. Physiol.*, 1987, **131**, 354–363.
- 50 J. S. Lee, S. Agrawal, M. von Turkovich, D. J. Taatjes, D. A. Walz and B. P. Jena, *J. Cell. Mol. Med.*, 2012, **16**, 945–949.
- 51 Z. Wang, J. Irianto, S. Kazun, W. Wang and M. M. Knight, *Osteoarthritis Cartilage*, 2015, **23**, 289–299.
- 52 E. O. Agbani, C. M. Williams, Y. Li, M. T. van den Bosch, S. F. Moore, A. Mauroux, L. Hodgson, A. S. Verkman, I. Hers and A. W. Poole, *JCI Insight*, 2018, **3**, e99062.
- 53 Y. Qiu, A. C. Brown, D. R. Myers, Y. Sakurai, R. G. Mannino, R. Tran, B. Ahn, E. T. Hardy, M. F. Kee, S. Kumar, G. Bao, T. H. Barker and W. A. Lam, *Proc. Natl. Acad. Sci. U. S. A.*, 2014, **111**, 14430–14435.
- 54 V. Tutwiler, R. I. Litvinov, A. P. Lozhkin, A. D. Peshkova, T. Lebedeva, F. I. Ataullakhanov, K. L. Spiller, D. B. Cines and J. W. Weisel, *Blood*, 2016, **127**, 149–159.
- 55 H. Demirin, H. Ozhan, T. Ucgun, A. Celer, S. Bulur, H. Cil, C. Gunes and H. A. Yildirim, *Thromb. Res.*, 2011, **128**, 358–360.
- 56 S. Handtke and T. Thiele, *J. Thromb. Haemostasis*, 2020, **18**, 1256–1267.
- 57 J. S. Cook, *J. Gen. Physiol.*, 1967, **50**, 1311–1325.
- 58 A. Connolly and H. G. Hempling, *Cryobiology*, 1985, **22**, 351–358.
- 59 W. J. Armitage and B. K. Juss, *J. Cell. Physiol.*, 1996, **168**, 532–538.
- 60 Z. M. Ruggeri and G. L. Mendolicchio, *Circ. Res.*, 2007, **100**, 1673–1685.
- 61 S. Vaiyapuri, C. I. Jones, P. Sasikumar, L. A. Moraes, S. J. Munger, J. R. Wright, M. S. Ali, T. Sage, W. J. Kaiser, K. L. Tucker, C. J. Stain, A. P. Bye, S. Jones, E. Oviedo-Orta, A. M. Simon, M. P. Mahaut-Smith and J. M. Gibbins, *Circulation*, 2012, **125**, 2479–2491.



- 62 R. Chen and N. Liang, *Cell Biol. Int.*, 1998, **22**, 429–435.
- 63 J. E. Fox, *Thromb. Haemostasis*, 1993, **70**, 884–893.
- 64 R. D. Allen, L. R. Zacharski, S. T. Widirstky, R. Rosenstein, L. M. Zaitlin and D. R. Burgess, *J. Cell Biol.*, 1979, **83**, 126–142.
- 65 M. J. Maxwell, S. M. Dopheide, S. J. Turner and S. P. Jackson, *Arterioscler., Thromb., Vasc. Biol.*, 2006, **26**, 663–669.
- 66 J. Hanke, D. Probst, A. Zemel, U. S. Schwarz and S. Köster, *Soft Matter*, 2018, **14**, 6571–6581.
- 67 A. K. Paknikar, B. Eltzner and S. Köster, *Prog. Biophys. Mol. Biol.*, 2019, **144**, 166–176.
- 68 M. Fritz, M. Radmacher and H. E. Gaub, *Exp. Cell Res.*, 1993, **205**, 187–190.
- 69 S. Posch, I. Neundlinger, M. Leitner, P. Siostrzonek, S. Panzer, P. Hinterdorfer and A. Ebner, *Methods*, 2013, **60**, 179–185.
- 70 B. Hechler, A. Dupuis, P. H. Mangin and C. Gachet, *Res. Pract. Thromb. Haemostasis*, 2019, **3**, 615–625.
- 71 Y. Liu, W. Wu, S. Feng, Y. Chen, X. Wu, Q. Zhang and S. Wu, *Microsyst. Nanoeng.*, 2023, **9**, 131.
- 72 E. Moendarbary, L. Valon, M. Fritzsche, A. R. Harris, D. A. Moulding, A. J. Thrasher, E. Stride, L. Mahadevan and G. T. Charras, *Nat. Mater.*, 2013, **12**, 253–261.
- 73 J. Rheinlaender and T. E. Schäffer, *Nanoscale*, 2019, **11**, 6982–6989.
- 74 C. Spagnoli, A. Beyder, S. Besch and F. Sachs, *Phys. Rev. E: Stat., Nonlinear, Soft Matter Phys.*, 2008, **78**, 031916.
- 75 C. Roffay, G. Molinard, K. Kim, M. Urbanska, V. Andrade, V. Barbarasa, P. Nowak, V. Mercier, J. García-Calvo, S. Matile, R. Loewith, A. Echard, J. Guck, M. Lenz and A. Roux, *Proc. Natl. Acad. Sci. U. S. A.*, 2021, **118**, e2103228118.
- 76 Y. Li and M. Guo, *Nat. Rev. Bioeng.*, 2024, **2**, 1023–1038.
- 77 P. A. Galie, P. C. Georges and P. A. Janmey, *Biochem. J.*, 2022, **479**, 1825–1842.
- 78 Z. Ilkan, J. R. Wright, A. H. Goodall, J. M. Gibbins, C. I. Jones and M. P. Mahaut-Smith, *J. Biol. Chem.*, 2017, **292**, 9204–9217.
- 79 E. Mammadova-Bach, T. Gudermann and A. Braun, *Arterioscler., Thromb., Vasc. Biol.*, 2023, **43**, 1339–1348.
- 80 M. Panova-Noeva, N. Arnold, M. I. Hermanns, J. H. Prochaska, A. Schulz, H. M. Spronk, H. Binder, N. Pfeiffer, M. Beutel, S. Blankenberg, T. Zeller, J. Lotz, T. Münzel, K. J. Lackner, H. Ten Cate and P. S. Wild, *Sci. Rep.*, 2017, **7**, 40229.
- 81 K. Pluta, K. Porębska, T. Urbanowicz, A. Gąsecka, A. Ołasińska-Wiśniewska, R. Targoński, A. Krasieńska, K. J. Filipiak, M. Jemielity and Z. Krasieński, *Biology*, 2022, **11**, 224.
- 82 G. Baidildinova, M. Nagy, K. Jurk, P. S. Wild, H. Ten Cate and P. E. J. van der Meijden, *Front. Cardiovasc. Med.*, 2021, **8**, 684920.
- 83 H. Lebas, K. Yahiaoui, R. Martos and Y. Boulaftali, *Front. Cardiovasc. Med.*, 2019, **6**, 132.

